Title

Chloride-Assisted Corrosion of Copper and Protection by Benzotriazole

Journal

ACS Applied Materials & Interfaces, 14(4)

ISSN

1944-8244

Authors

Yang, Shanshan
Zhao, Xiao
Qi, Zhiyuan
et al.

Publication Date

2022-02-02

DOI

10.1021/acsami.1c15808

Peer reviewed

Supplementary information

Chloride Assisted Corrosion of Copper and Protection by Benzotriazole

Shanshan Yang [1], Xiao Zhao [1,3], Zhiyuan Qi [1], Yi-Hsien Lu [1], Gabor Somorjai [1,2], Peidong Yang [1,2], Artem Baskin [4], David Prendergast [4], Miquel Salmeron [1,3,]*

[1] Materials Sciences Division, Lawrence Berkeley National Laboratory, Berkeley, California 94720, United States.

[2] Department of Chemistry, University of California-Berkeley, Berkeley, California 94720, United States.

[3] Department of Materials Science and Engineering, University of California-Berkeley, Berkeley, California 94720, United States.

[4] Molecular Foundry Division, Lawrence Berkeley National Laboratory, Berkeley, California 94720, United States.

[*] Corresponding author: MBSalmeron@lbl.gov

S6. XRD characterization for thermal evaporated Cu film

S7. SFVS check of the BTAH signal absorbed on CaF_2 window

S1. Sum frequency vibrational spectroscopy setup S-1

The beam orientations in all the SFVS experiments were: 45˚ for the 532 nm beam, and 56˚ for the mid-infrared beam, with respect to the perpendicular plane (reference plane). The polarization combination used in this work was SSP (S-polarized light for the SF output and for the input visible beam, and P-polarized light for the input infrared beam). The SF beam was collected by a Hamamatsu photon-multiplier tube (model R922). We used multiple irises along the calculated SF beam path (according to the phase matching equation) and several low-pass filters in order to minimize 532 nm stray light.

S2. Orientation check of the BTAH molecules absorbed to copper surface

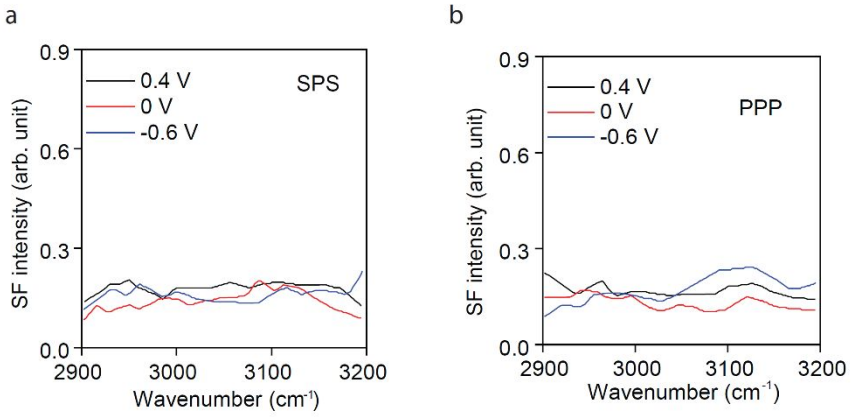

Figure S1 SPS (**a**) and PPP (**b**) SF spectra of BTAH at copper surface with 7 mM bulk concentration. The surface has reached saturation point for BTAH adsorption.

S3. *Ex situ* AFM, KPFM, XPS characterization for Cu-BTAH samples

To complement the information provided by SFVS, structural and chemical characterization of the Cu surface was performed ex situ, after removing the sample from the electrochemical cell at specific values of the potential. Topographic and electronic structural characterization of the Cu samples was achieved outside the solution by AFM and KPFM in an MFP-3D Asylum Research system, using conductive Pt/Ir

tips. The AFM cantilever holding the tip was mechanically oscillated at its 75 kHz resonance frequency and simultaneous modulated with a 2 kHz AC bias of 3.5V amplitude. Simultaneous topographic and tip-sample contact potential difference (CPD) were obtained in single-pass mode with side-band detection, to improve the spatial resolution.

Chemical characterization was obtained also ex situ by XPS in ultrahigh vacuum (~10−10 mbar) using a Thermo Fisher Scientific XPS/UPS system with a monochromatic Al Kα X-ray source (1486.6 eV).

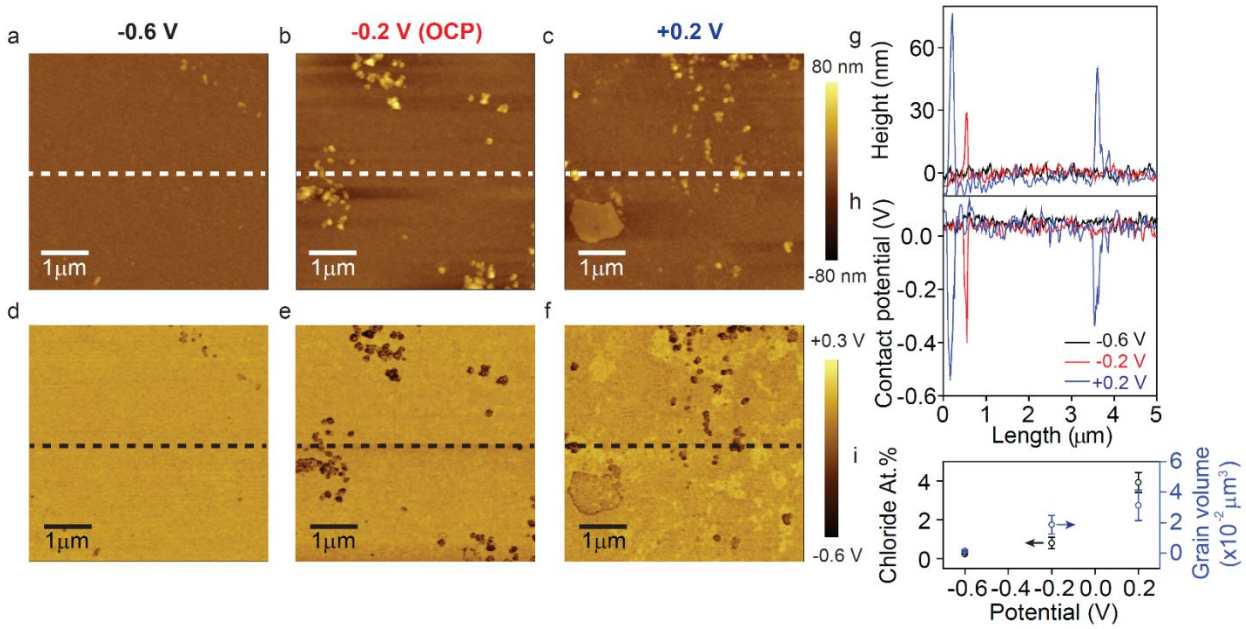

Figure S2 (**a**), (**b**) and (**c**) 5 μm × 5 μm AFM topographic images of the Cu sample after emersion from a 7 mM BTAH + 0.5 M NaCl solution at different potential -0.6 V, -0.2 V and 0.2 V, respectively. (**d**), (**e**) and (**f**) corresponding contact potential difference (CPD) maps. (**g**) Height profiles along the broken line in (a), (b) and (c). The surface roughness is ~3 nm over most of the surface, but additional protrusions with heights ranging from 10 to 30 nm appeared at the OCP (b), and higher anodic potentials (c), due to the corrosion reaction. (**h**) CPD profiles along the same broken line in (d), (e) and (f). The CPD changes to large negative values over the protrusions in (g) indicative of a different chemical composition there. (**i**) Atomic concentration (At.%) of Cl (left y-axis) determined by XPS and protrusion volume measured in KPFM (righ y-axis), as a function of potential.

We investigated how the surface topography and composition changed as a function of potential bias by acquiring AFM and KPFM images ex situ, as shown in Fig. S2. The images, topographic (a, b, c) and CPD (d, e, f) respectively, were acquired in air after emersion of the Cu sample from the solution containing 7

mM BTAH and NaCl at -0.6 V, -0.2 V (OCP) and 0.2 V. The image at -0.6 V shows a relative uniform surface with 3 nm rms roughness (Fig. S2a), and uniform CPD (Fig. S2d). Increasing the potential to -0.2 V resulted in the formation of protrusions up to 30 nm high (Fig. S2b), while after reaction at 0.2 V the protrusions became higher (40 to 80 nm, Fig. S2c). The CPD in the protrusions is substantially more negative than in the flat areas by -0.3 V to -0.5 V (Fig. S2h), indicating that the chemical composition there is different from that in the uniform substrate, where the contact potential remained unchanged.

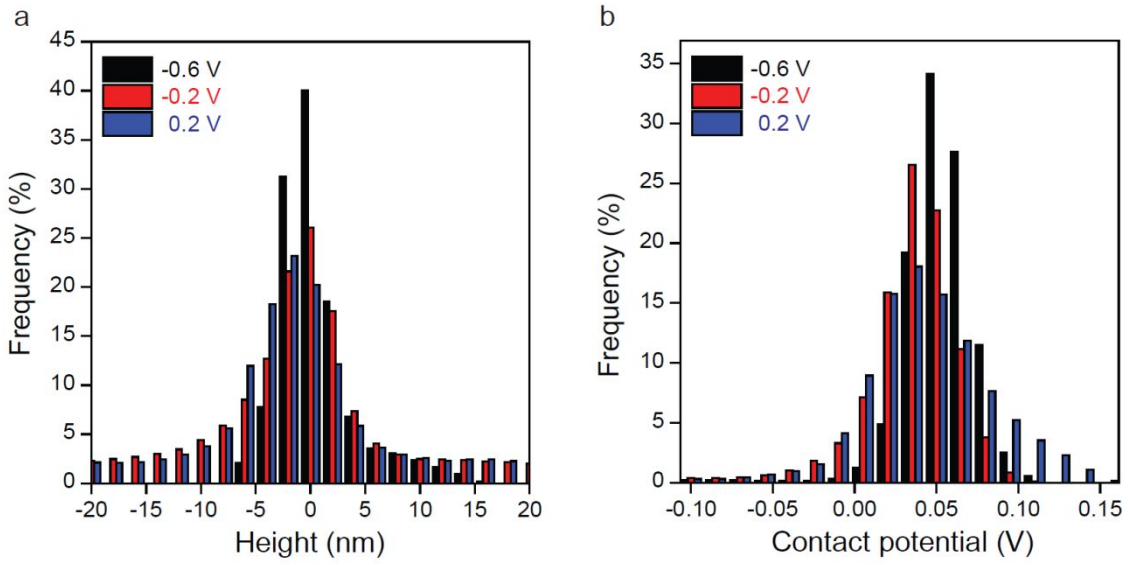

Figure S3 (**a**) and (**b**) AFM height and contact potential histograms of the Cu sample after emersion from a 7 mM BTAH + 0.5 M NaCl solution at different potential -0.6 V (black), -0.2 V (red) and +0.2 V (blue), respectively.

ELEMENT	BINDING ENERGY	AT% (-0.6V)	AT% (-0.2V)	AT% (+0.2V)
O *1s*	531.08	8.99	11.85	18.81
C *1s*	285.08	75.27	71.15	60.88
N *1s*	400.08	9.99	8.39	7.38
Cu *2p 3/2*	932.08	5.51	7.81	9.02
Cl *2p*	199.08	0.24	0.8	3.91

Table S1 Elements detected by XPS and their atomic concentration (AT%) corrected by the relative sensitivity factor and mean free path of the corresponding photoelectrons, which vary between 17 and 10 Å approximately. The three samples studied were extracted from the solution at -0.6 V, -0.2 V and +0.2 V, respectively, in Fig. S2a-c.

The chemical nature and composition of the surface layers formed from a 7 mM BTAH + 0.5 M
solution was analyzed by XPS after extraction of the sample at potentials of -0.6 V, -0.2 V and 0.2 V. The results, shown in Table S1, indicate that all the samples contain oxygen (O), carbon (C), nitrogen (N), and chloride (Cl), in addition to Cu from the substrate. The C peak likely contains small contributions from initial adventitious C. Oxygen increased by a factor of roughly 2 although some amount could be present from the start after sample preparation and/or by exposure to air after extraction and additionally increased as a result of corrosion. The Cl increased most dramatically by a factor of 16. The concentrations of Cl changed in line with the AFM observations showing that the grain volume of the protrusions in the topographic images of Fig.S2a-c are correlated with the Cl atomic concentration measured by XPS (Fig. S2i).

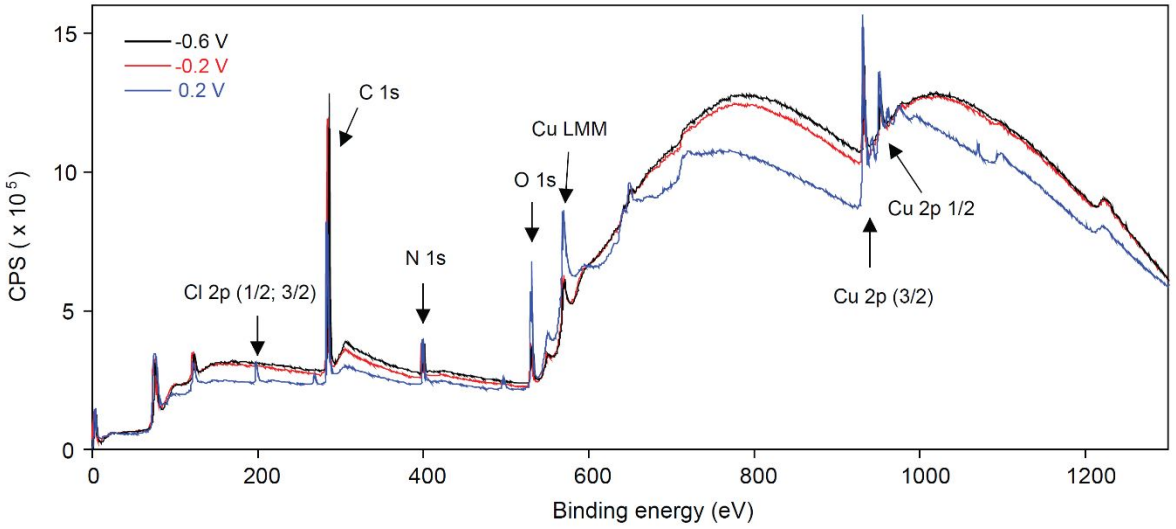

Figure S4 XPS survey spectra

S4. SF spectra used to deduce the Gibbs adsorption energy for BTAH molecule and Cl-

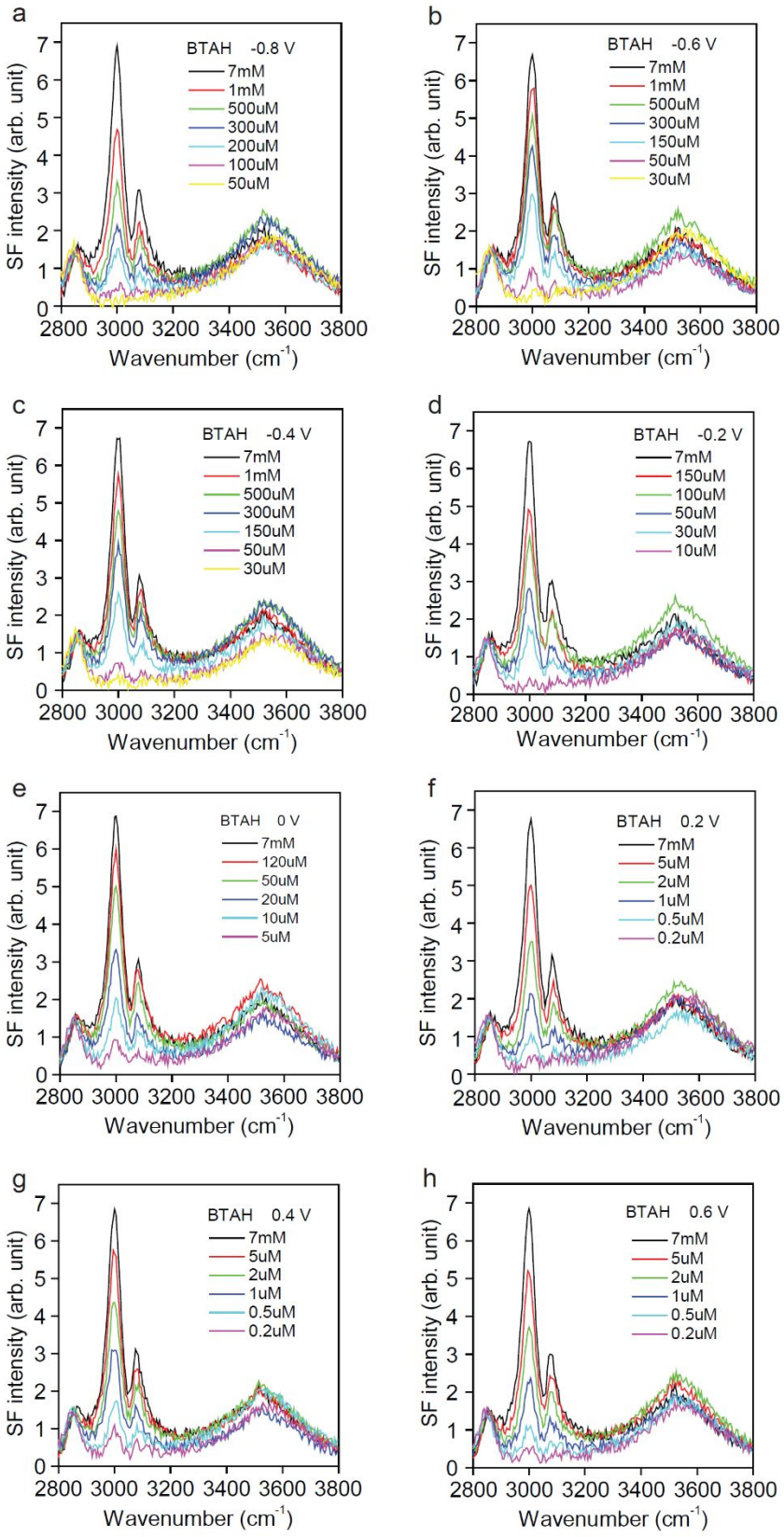
a
BTAH -0.8 V
7mM
1mM
500uM
300uM
200uM
100uM
50uM
b
BTAH -0.6 V
7mM
1mM
500uM
300uM
150uM
50uM
30uM
c
BTAH -0.4 V
7mM
1mM
500uM
300uM
150uM
50uM
30uM
d
BTAH -0.2 V
7mM
150uM
100uM
50uM
30uM
10uM
e
BTAH 0 V
7mM
120uM
50uM
20uM
10uM
5uM
f
BTAH 0.2 V
7mM
5uM
2uM
1uM
0.5uM
0.2uM
g
BTAH 0.4 V
7mM
5uM
2uM
1uM
0.5uM
0.2uM
h
BTAH 0.6 V
7mM
5uM
2uM
1uM
0.5uM
0.2uM
SF intensity (arb. unit)
Wavenumber (cm-1)
2800 3000 3200 3400 3600 3800
0 1 2 3 4 5 6 7

Figure S5 SF spectra from the copper/BTAH interface with different BTAH bulk concentrations at (**a**) -0.8 V, (**b**) -0.6 V, (**c**) -0.4 V, (**d**) -0.2 V, (**e**) 0.0 V, (**f**) 0.2 V, (**g**) 0.4 V, (**h**) 0.6 V, in a buffer solution of 0.5 M $NaClO_4$, respectively. The constant value of the frequency of the CH peaks and of their intensity ratio indicates that the changes in intensity are due only to changes in coverage of BTAH.

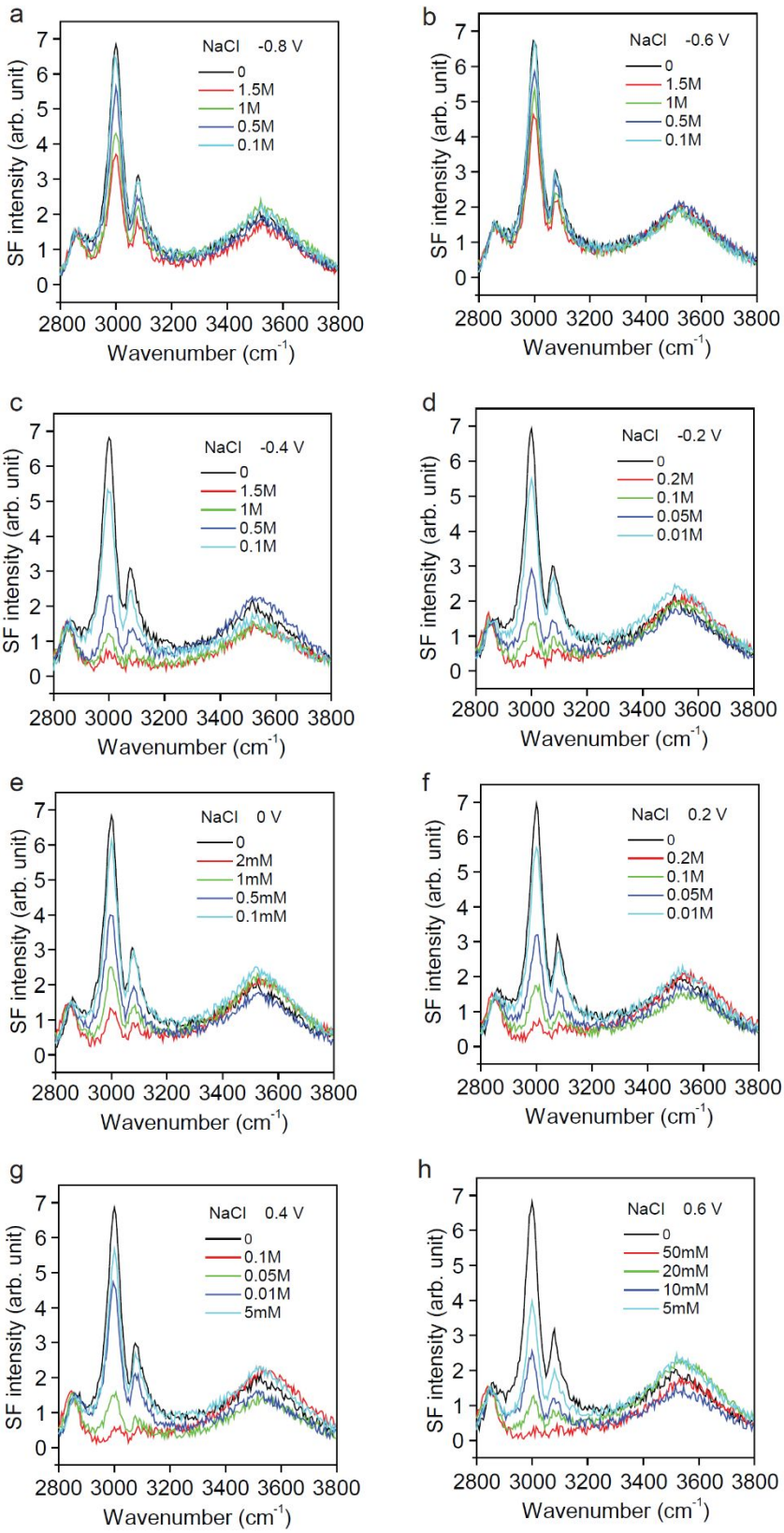
a
NaCl -0.8 V
0
1.5M
1M
0.5M
0.1M
b
NaCl -0.6 V
0
1.5M
1M
0.5M
0.1M
c
NaCl -0.4 V
0
1.5M
1M
0.5M
0.1M
d
NaCl -0.2 V
0
0.2M
0.1M
0.05M
0.01M
e
NaCl 0 V
0
2mM
1mM
0.5mM
0.1mM
f
NaCl 0.2 V
0
0.2M
0.1M
0.05M
0.01M
g
NaCl 0.4 V
0
0.1M
0.05M
0.01M
5mM
h
NaCl 0.6 V
0
50mM
20mM
10mM
5mM
SF intensity (arb. unit)
Wavenumber (cm-1)
2800 3000 3200 3400 3600 3800

Figure S6 SF spectra of copper/BTAH/NaCl interface with fixed 7 mM of BTAH and different concentrations of Cl^- ions in solution at (**a**) -0.8 V, (**b**) -0.6 V, (**c**) -0.4 V, (**d**) -0.2 V, (**e**) 0.0 V, (**f**) 0.2 V, (**g**) 0.4 V, (**h**) 0.6 V, in a buffer solution of 0.5 M $NaClO_4$, respectively.

S5. SDS surface density calculation

The normalization was done through the amplitude ratio of the methyl group at 2880 cm^{-1} between the sample of 1mM SDS + 1 mM BTAH/copper and the saturated SDS layer/copper interface. For SDS spectra, there are 3 main features, methylene group symmetric stretching (CH_2-ss) at 2850 cm^{-1}, and methyl group symmetric stretching (CH_3-ss) at 2880 cm^{-1} as well as methyl group Fermi resonance (CH_3-FR) at 2935 cm^{-1}. The presence of CH_2-ss mode indicates that there are defects like gauche defects in the backbone of alkane chain of SDS, while the weak antisymmetric stretching peak (CH_3-as) at 2960 cm^{-1} indicates that a majority of methyl groups are inclined pointing upwards along the surface normal since the net vibration vector of symmetric and antisymmetric stretching modes of methyl group are orthogonal to each other. However, if the CH_3 group is tilted on the surface, both modes should be dominant the spectra. Thus, although the alkyl chains might be somewhat disordered, we use the fitting amplitude of the methyl group at 2880 cm^{-1} to make a rough estimate of the relative surface coverage of SDS in sample of 1mM SDS + 1 mM BTAH.

The measured spectra were fitted by the following expression:

$$\chi^{(2)}_{S,eff}(\omega) = \chi^{(2)}_{NR,eff} + \sum_q \frac{A_q}{\omega - \omega_q + i\Gamma_q} \quad \text{(S1)}$$

where $\chi^{(2)}_{NR,eff}$ is the non-resonant background, ω_q and A_q is the resonant mode frequency and amplitude, and Γ_q is the damping constant. For the case of SDS, we tried to use two different fitting methods to compare the possible variance between them, that is, (1) global fitting, (Fig. S7 dashed lines and Tab. S2 below) in which two curves share the same parameters except the amplitude; (2) fitting two curve separately, (Fig. S7 solid lines and Tab. S3 below) in which we fitted the parameters separately except the shared peak positions. The intensity amplitudes at 2880 cm^{-1} of 1 mM SDS + 1 mM BTAH and that of SDS saturation on copper is BTAH are 3.35/33.97 ≈ 0.098 for global fitting and 4.94/36.48 ≈ 0.135 for fitting separately, which means that the surface coverage of SDS is in the range of 9.8% -13.5% for the 1mM SDS + 1 mM BTAH sample. We acknowledge that this is a rough estimation, since the configuration of SDS on copper is hard to ascertain.

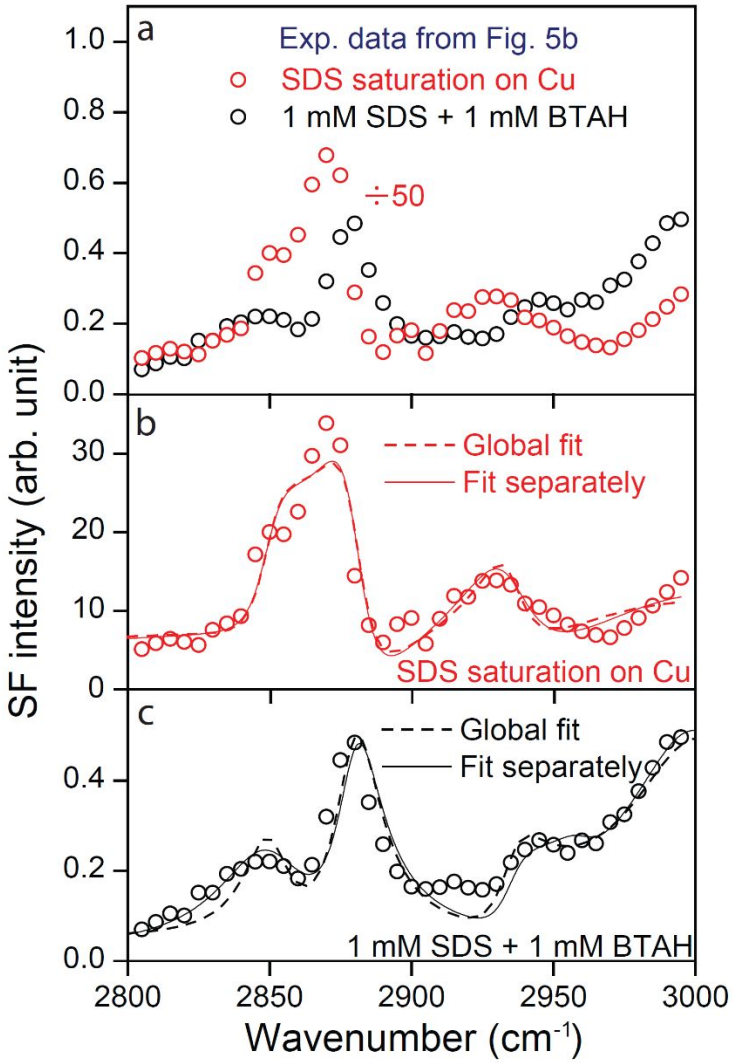

Figure S7 Fitting of SDS (a) Experiment data from 2800 – 3000 cm^{-1} of figure 5b of the main text. SF spectrum of adsorbed SDS and BTAH on copper in 0.5 M NaCl solution (b) and SDS spectrum on the copper surface at saturation for SDS adsorption (c). Dashed line for global fitting and solid line for fitting two curves separately.

Mode	Peak position (ω_q, cm^{-1})	Amplitude (A_q)	damping constant (Γ_q)
CH_2-ss	2850	2.3 / -18.7	10.65
CH_3-ss	2880	3.5 / 33.97	9.45
CH_3-FR	2935	2.2 / 16.9	9.48

CH_3-as	2960	- 0.005 / - 0.015	10.21

Table S2 (global fitting) Fitting parameter for the SDS curves in Fig. 5b in the main text. Two curves share the same parameter except the amplitude shown in black numbers for 1mM SDS + 1 mM BTAH and blue for SDS saturation on copper.

Mode	**Peak position (ω_q, cm^{-1})**	**Amplitude (A_q)**	**damping constant (Γ_q)**
CH_2-ss	2850	7.47 / -17.78	15.74/9.65
CH_3-ss	2880	4.94 / 36.48	9.73/9.35
CH_3-FR	2935	1.7 /33.15	9.28/14.78
CH_3-as	2960	- 0.24 / - 0.64	9.82/10.45

Table S3 (Fitting separately) Fitting parameter for the SDS curves in Fig. 5b in the main text. Two curves share the same parameters, except the shared peak positions. The amplitude and damping parameters are shown in black for 1mM SDS + 1 mM BTAH and blue for SDS saturation on copper.

S6. XRD characterization for thermal evaporated Cu film

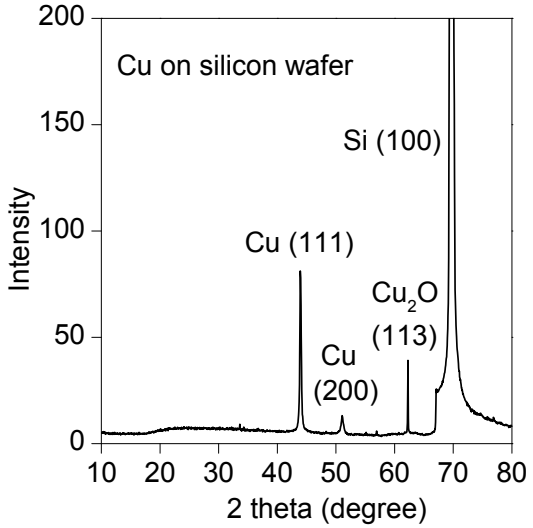

Fig. S8 XRD of copper film on silicon wafer

From the XRD results shown above, there are two orientations present on the surface, Cu (111) and Cu (200). The intensity indicates that Cu (111) is the dominant orientation of our copper film. The peaks of copper oxide are formed during transferring from the evaporator to the XRD setup. The peak from silicon substrate is also present in the figure.

S7. SFVS check of the BTAH signal absorbed on CaF_2 window

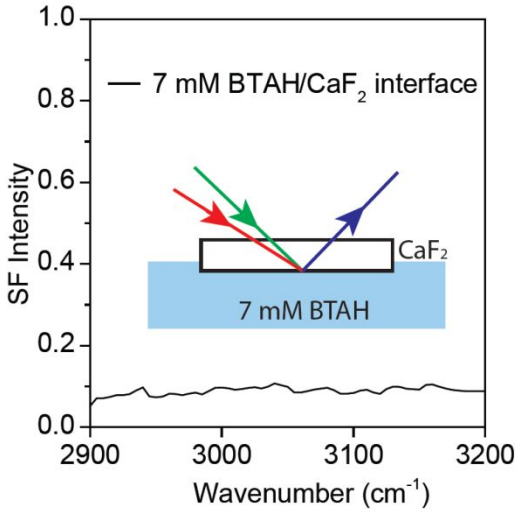

Fig. S9 SF signal of BTAH adsorbed on CaF_2 window

For signal of BTAH adsorbed on CaF_2 window, we checked the spectra without copper beneath. There is no observable signal from the interface of BTAH/CaF_2 window. The experimental setup and spectral results are depicted in Fig. S9.